ELSEVIER

Journal of Biomechanics 40 (2007) 1813–1823

JOURNAL OF BIOMECHANICS

www.elsevier.com/locate/jbiomech
www.JBiomech.com

Predicting fracture of the femoral neck

Leonard Stepanskiy, Rahamim (Rami) Seliktar*

School of Biomedical Engineering, Science and Health Systems, Drexel University, Philadelphia, PA 19104, USA

Accepted 26 July 2006

Abstract

A prediction of the probability of safe loading of the femoral neck, based on queueing theory, is presented. The following methods have been applied: (I) criterion of bone fracture was formulated, taking into consideration the complex state of stress–strain in the porosity zones of the bone; (II) tensile stresses around pores in the stretched zone of the bone were evaluated; (III) the influence of random events of the critical regimes of loading was modeled.

The evaluation of the probability of safe loading of bones was obtained based on the levels of the tensile stresses, Young's moduli and ultimate tensile stresses which are affected by the increase in bone porosity and the distribution of the pores. Examples of analysis involving typical mechanical properties of bone in areas of vascular and lacunar–canalicular porosity are demonstrated.

The ranges of initial average values of effective Young's moduli and ultimate tensile strengths were taken as 15.8–17.5 GPa and 83–95 MPa, respectively.

The present analysis discovers the existence of three levels of safe loading: (1) a relatively safe level of the nominal tensile stresses (smaller than (2.8–3.2) MPa) where the probability of safe loading is of the order of 0.95 for the bone porosity which is less than 0.15; (2) an intermediate level of safety where the nominal tensile stresses are below (4.2–4.8) MPa and the probability of safe loading is 0.89 or higher, for the same level of bone porosity; (3) a critical level of safe loading where the nominal tensile stresses are about (8.3–9.5) MPa; they lead to sharp drop of probabilities of safe loading to 0.85–0.8 if the porosity is about 0.10 and to probabilities of 0.41–0.4 if the porosity is about 0.15.

Keywords: Bone; Hip injury; Bone mechanics; Fracture risk

1. Introduction

Femoral neck fractures are common injuries and constitute a major morbidity and mortality factor among the elderly (women in particular). A wealth of related literature is available, such as: Kanis et al. (2002), Kanis (2002a, b), Crabtree et al. (2002), Brazier et al. (2002), Kartoge et al. (2003) and Mayhew et al. (2005).

The biomechanical conditions that are responsible for hip fractures in the elderly are somewhat unclear (Duboeuf et al., 1997). Undoubtedly, bone fragility and susceptibility to trauma play a major role in its failure. It is therefore important to determine what is the critical level of porosity beyond which bone fragility reaches a dangerous level (Cummings et al., 1993). To date there have been many works focusing on the relationships between mechanical and morphological properties of human trabecular bone (Cowin, 1999; Smit et al., 2002; Zysset, 2003; Morgan et al., 2003; Norman et al., 1995; Rajapakse et al., 2004; Homminga et al., 2003; Dong and Guo, 2004). Typical schemes of loading of the proximal femur are discussed by Bagge (2000) and Testi et al. (1999, 2002). A stress–strain analysis of the loaded femur, using finite elements has been considered in numerous works such as: Wirtz et al. (2003), Testi et al. (2002, 2004), Keyak and Rossi (2000) and Ota et al. (1999). Some fracture criteria of bones and applications of linear fracture mechanics for analysis of bone raptures are discussed by Duboeuf et al. (1997), Pietruszczak et al. (1999), Malik et al. (2003), Yeni and Fyhrie (2003), Keyak and Rossi (2000) and Nalla et al. (2005). Fatigue behavior of trabecular bone is considered by Haddock et al. (2004), Currey (2004), Ganguly et al. (2004), Dargent-Molina et al. (1996), Zioupos and Currey

*Corresponding author.
E-mail address: seliktar@Drexel.edu (R.R. Seliktar).

0021-9290/$ - see front matter © 2006 Published by Elsevier Ltd.
doi:10.1016/j.jbiomech.2006.07.002

(1998), Kanis et al. (2002), Crabtree et al. (2002), Kartoge et al. (2003) and Mayhew et al. (2005), analyzed numerous random factors influence both loading of the femoral neck and its fragility, especially in the elderly. These factors may be separated into several groups: (i) factors concerned with the levels of loading; (ii) factors based on the sites and directions of action of the loads; (iii) morphometric and densitometric factors; (iv) factors involving bone mineral distribution. The intensity of influence of random factors is affected by age, gender, weight, race, physical activity, food, and environment.

We conclude from previous studies that the quality of prediction of the risk of fracture of the femoral neck depends on efficiency of the used criterion of fracture and its association with influence of the main random factors. It is noteworthy, however, that the criteria proposed in the relevant literature are not conclusive and correspond only weakly to the experimental observations.

The objective of the present work is to develop a method of prediction of the probability of fracture in the femoral neck, which accounts for: (i) the level of the tensile stresses; (ii) the decrease of Young's modulus and the ultimate tensile stress with the increase of bone porosity; (iii) the distribution of the pores; (iv) the influence of the random events. To achieve this objective the following problems were solved:

(I) criterion of bone fracture was developed, which takes into account the observed features of fracture, namely action of tensile stresses and threshold of work done by the tensile stresses;
(II) evaluation of the concentration of the tensile stresses around pores in the stretched zone of the bone;
(III) evaluation of the probability of safe loading of bone by simulation of loading in the porosity site, using queueing systems (QSs), so as to account for the influence of the random events on the relationship between critical levels of nominal tensile stresses, bone porosity and the reduction of bone strength with the increase of bone porosity.

2. Methods

2.1. The critical state of stress–strain in bones leading to failure

In order to evaluate the state of stress–strain that produced bone fractures the following assumptions were made. The concept of Wolf's Law of Bone Remodeling was adopted as a governing law in the formation and remodeling of trabecular bone. The relevant bone material in the femoral head–neck and the epyphisial region is homogeneous, isotropic, elastic–viscous–plastic material (see Appendix A).

Bone failure may only occur in regions, where tensile stresses act. At first all these regions undergo bending or torsion.

The criterion of bone fracture should satisfy the experimentally observed characteristics of bone fracture: (i) action of tensile stresses; (ii) large plastic strains if the acting tensile stresses are not high; (iii) small plastic deformation if the acting tensile stresses are high; (iv) decrease of the ultimate plastic strains before fracture, if the tensile stresses act along two or three axes. This criterion must facilitate prediction of fracture by using the results of traditional mechanical tests in tension, bending and torsion. If the deformed material can be assumed isotropic until fracture, then the above conditions are satisfied by the assumption of constancy of the work done by tensile stresses on the equivalent plastic strains:

$$W_1 + W_2 + W_3 = [W] = \text{const.} \tag{1}$$

Here $[W]$ is the ultimate value of a total work done in a unit volume by the tensile stresses on the equivalent plastic strains; W_1, W_2, W_3 are the works done in unit of volume on the equivalent plastic strains, by the maximum, median and minimum tensile stresses denoted by: $\sigma_1^+, \sigma_2^+, \sigma_3^+$, that act in three mutually perpendicular directions 1, 2, 3. The terms W_1, W_2, W_3 are equal to:

$$W_1 = \int_0^{e_{\text{eq}}^*} \sigma_1^+ \, \mathrm{d}e_{\text{eq}},$$

$$W_2 = \int_0^{e_{\text{eq}}^*} \sigma_2^+ \, \mathrm{d}e_{\text{eq}},$$

$$W_3 = \int_0^{e_{\text{eq}}^*} \sigma_3^+ \, \mathrm{d}e_{\text{eq}}. \tag{2}$$

Here e_{eq}^* is the final value of the equivalent plastic strain e_{eq}. Prediction of failure according to assumption (1) is compared to known experimental results of mechanical tests in tension, torsion and bending (Appendix E). Accounting for the difference of ultimate plastic strains of tested specimens harvested from bone and cut in different directions, equality (1) changes into the following energetic criterion of bone fracture:

$$W_1/[W]_1 + W_2/[W]_2 + W_3/[W]_3 = 1. \tag{3}$$

Here $[W]_1$, $[W]_2$, $[W]_3$ are the ultimate values of works corresponding to W_1, W_2, W_3, respectively.

According Hook's law the critical equivalent stress $[\sigma_{\text{eq}}]$ that causes failure in unit of bone volume is described by the following expression (see Appendix A):

$$[\sigma_{\text{eq}}] = \left[\frac{4E_{\text{eff}}\sigma_{\text{Y}}^2}{(1+\nu)(\beta_1/[W]_1 + \beta_2/[W]_2 + \beta_3/[W]_3)}\right]^{0.25}. \tag{4}$$

Here E_{eff} is the effective Young's modulus (see Appendix A):

$$E_{\text{eff}} = \frac{2(1+\nu)\sigma_{\text{eq}}}{3\varepsilon_{\text{eq}}}\left[1 + \left(3\mu\frac{\varepsilon_{\text{eq}}}{\sigma_{\text{eq}}} + \frac{\varepsilon_{\text{eq}}}{\dot{\varepsilon}_{\text{eq}}}\right)\Big/ t\right], \tag{5}$$

where ν is the median value of Poisson's ratio; σ_{eq}, ε_{eq}, $\dot{\varepsilon}_{\text{eq}}$, are the equivalent stress, the equivalent strain and the equivalent strain rate, respectively; t is the loading time; μ is the median dynamic coefficient of viscosity; σ_{Y} is the

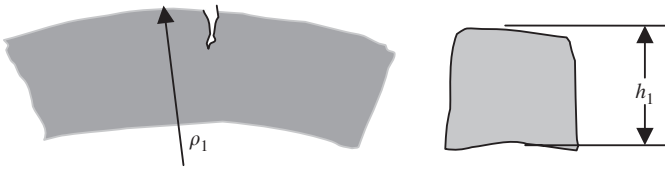

Fig. 1. Schematic description of a broken specimen after its bending.

median value of the yield tensile strength; β_1, β_2, β_3 are median values of the following ratios: $\beta_1 = \sigma_1^+/\sigma_{eq}$; $\beta_2 = \sigma_2^+/\sigma_{eq}$; $\beta_3 = \sigma_3^+/\sigma_{eq}$, during loading of the bone.

The values $[W]_1$, $[W]_2$, $[W]_3$ may be obtained from the results of bending of specimens (Draper and Goodship, 2003). These specimens should be cut out from the critical region of the bones so that the axes of the specimens directed along their lengths were parallel to the above directions 1, 2, 3 (see Appendix C):

$$[W]_1 \approx \frac{\sigma_{b1} h_1}{4(\rho_1 - 0.5h_1)},$$
$$[W]_2 \approx \frac{\sigma_{b2} h_2}{4(\rho_2 - 0.5h_2)},$$
$$[W]_3 \approx \frac{\sigma_{b3} h_3}{4(\rho_3 - 0.5h_3)}. \quad (6)$$

Here σ_{b1}, σ_{b2}, σ_{b3}, are the ultimate tensile strengths of specimens bent in planes parallel to the directions 1, 2, 3, respectively, h_1, h_2, h_3 are the initial heights of those specimens; ρ_1, ρ_2, ρ_3 are the radii of the curvature of the outer surfaces of these specimens at the onset of failure (Fig. 1).

2.2. The effect of porosity

Let α be the initial value of bone porosity, χ is the actual bone porosity, E_{eff0}, σ_{b10}, σ_{b20}, σ_{b30} are the initial values of E_{eff}, σ_{b1}, σ_{b2}, σ_{b3}, respectively, ρ_{10}, ρ_{20}, ρ_{30} are the initial values of the radii ρ_1, ρ_2, ρ_3, respectively. According to numerous studies (Cowin, 1999; Crabtree et al., 2002; Morgan et al., 2003; Smit et al., 2002; Kabel et al., 1999), changes of strength and stiffness of bones with evolution of osteoporosis are similar to changes which are described by exponential functions. Considering the decrease of E_{eff}, σ_{b1}, σ_{b2}, σ_{b3} from their initial values and increase of radii ρ_1, ρ_2, ρ_3 from their initial values, with the increase of bone porosity above its initial value α, the new values are described by the following expressions:

$$E_{eff} = E_{eff0} \exp[-c_1(\chi - \alpha)], \quad (7)$$

$$\sigma_{b1} = \sigma_{b10} \exp[-c_2(\chi - \alpha)],$$
$$\rho_1 = \rho_{10} \exp[c_5(\chi - \alpha)], \quad (8)$$

$$\sigma_{b2} = \sigma_{b20} \exp[-c_3(\chi - \alpha)],$$
$$\rho_2 = \rho_{20} \exp[c_6(\chi - \alpha)], \quad (9)$$

$$\sigma_{b3} = \sigma_{b30} \exp[-c_4(\chi - \alpha)],$$
$$\rho_3 = \rho_{30} \exp[c_7(\chi - \alpha)]. \quad (10)$$

Here $c_1, \ldots, c_7$ are positive constants, depending on age, gender, initial and actual non-homogeneity of distribution of minerals, organic components and bone fluid.

Sensitivity of the assessments in (7)–(10) to small changes in $c_1, \ldots, c_7$ is linearly proportional to the difference $(\chi - \alpha)$. For E_{eff}, σ_{b1}, σ_{b2}, σ_{b3} such sensitivity of the corresponding assessments decreases exponentially with increase of the product of $c_1, \ldots, c_4$ and $(\chi - \alpha)$. For the radii ρ_1, ρ_2, ρ_3, such sensitivity decreases exponentially with the growth of the product of $c_5, \ldots, c_7$ and $(\chi - \alpha)$.

To define the constants $c_1, \ldots, c_4$ some published results related to the relationships between bone strength and bone porosity (Crabtree et al., 2002; Currey, 2004; Morgan et al., 2003; Zioupos and Currey, 1998) were substituted into the expressions (7)–(10). The results show ranges of the constants $c_1, \ldots, c_4$ to be of the order of 7–12.

2.3. Evaluation of the tensile stresses in the porous bone region

To estimate the values of the tensile stresses around the pore in the porous region of the bones the following assumptions were made: the most dangerous positions of the pores leading to fractures are the positions in the stretched zones of the bones (Figs. 2 and 3); three regions of the statically admissible stresses exist around the pore:

(i) Region 1: the area between the contour of the pore's section and the circumscribed circle with radius a; in this region the state of stress can be considered a planar uniform compression corresponding to the pressure q_F of the bone fluid.
(ii) Region 2: a ring-shape with an inner radius a and outer radius $R = \min(S_s, 0.5S_r)$, where S_r is the average distance between the centers of the circles circumscribing the contour of the pores; S_s is the average distance between the center of the circle circumscribing the contour of the pore and the contour

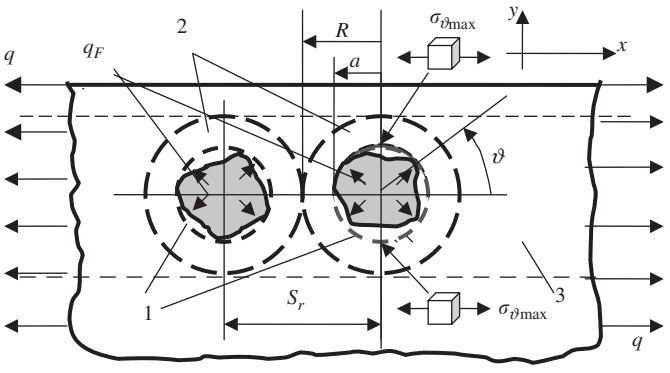

Fig. 2. Proposed scheme of positions of pores in the inner zone of the acting tensile stresses.

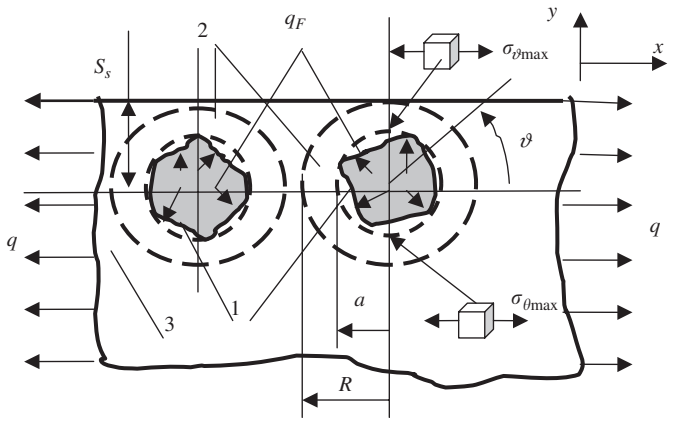

Fig. 3. Proposed scheme of positions of pores in the outer zone of the acting tensile stresses.

of the stretched surface of the bone in the section parallel to the plane of the bending.

(iii) Region 3: the outer region of the stripe shape with width equal to $2R$. Here the state of stress is a plane state of stress, defined by the nominal tensile stresses q, where the value of q is

$$q = T/2R, \tag{11}$$

where T is the tensile load in the part of the bone that corresponds to the stripe of a width $2R$ and a unit of the thickness.

The calculations of the statically admissible stresses in Appendix D estimate the maximum tensile stresses σ_1^+ which are circumferential stresses $\sigma_{\vartheta\max}$ acting in the elementary volumes at the ends of the diameter of the circumscribed circle, where $r = a$; $\vartheta = \pm\pi/2$. These sites are at higher risk of failure.

Assuming that in these critical sites of the bone $\sigma_Y \approx 0.95\sigma_{b1}$ and the tensile stresses σ_2^+, σ_3^+ are negligible, terms β_2 and β_3 in the expression (4) are $\beta_2 = \beta_3 = 0$. Then equivalent stresses in these sites are $\sigma_{eq} \approx \sigma_1^+ = \sigma_{\theta\max}$. The corresponding substitutions in the equalities (4) and (6) and their combination define the limited equivalent stress $[\sigma_{eq}]$.

2.4. The probability of safe loading of the femoral neck

To take into account the influence of random events on the bone fracture, the following assumptions were made: the streams of the random events that lead to loading and to fracture of the bone are simple Markov's streams of the random events, i.e. the stationary streams, the ordinary streams and memory-less streams (Saaty, 1961; Gross and Harris, 1985). The loading of the femoral neck and its damage are similar to serving of the requirements in the open QS with refusals and channels for the service. In such QS (see Appendix B) the femoral neck is the requirement to the service. The loading of the bone is the current service of the requirement. If loading of the bone leads to the fracture of the femoral neck, it means satisfaction of the service requirements. The number of channels for the service is equal to an amount of the critical zones in bone structure. The graph of the possible states of the considered QS is presented in Fig. 4. The state 0 is either the state of the readiness of the bone to the loading or the state of the fracture of the bone in the first of the critical zones. State 1 is either the state of the loading of the bone in the first of the critical zones or the state of the fractures in two critical zones. State 2 is either the state of the loading of the bone in two critical zones or the state of the fracture in three critical zones. The state k is the state of the loading of the bone in all k critical zones but there are no channels when the fracture occurs.

Assume the following: the intensities of the streams of the random events that carry QS from the states 0 to 1, from states 1 to 2, from states $k-1$ to k are equal to

$$\lambda_{0.1} = \lambda_{1.2} = \cdots = \lambda_{k-1.k} = C/\sigma_{eq}, \tag{12}$$

where σ_{eq} is the equivalent stress corresponding to the loading, C is a constant. The intensity of the streams of the random events that carry QS from states 1 to 0 is equal to

$$\lambda_{10} = p_{[\sigma]}C/[\sigma_{eq}], \tag{13}$$

where $[\sigma_{eq}]$ is the limited equivalent stress, $p_{[\sigma]}$ is the probability of approaching the limited equivalent stress $[\sigma_{eq}]$ by the equivalent stress σ_{eq}. Let us accept that

$$p_{[\sigma]} = W_{\sigma_{eq}}/W_{[\sigma_{eq}]} \approx \sigma_{eq}^2\Big/[\sigma_{eq}]^2, \tag{14}$$

where $W_{\sigma_{eq}}$ and $W_{[\sigma_{eq}]}$ are the specific works done by the stresses σ_{eq} and $[\sigma_{eq}]$, respectively, and $W_{\sigma_{eq}} \leqslant W_{[\sigma_{eq}]}$. The intensity of the streams of the random events that carry QS from states 2 to 1 is equal to $\lambda_{2.1} = 2\lambda_{10}$, because the service in state 2 fulfills two channels. The intensity of the streams of the events that carry QS from the state k to the state $k-1$ is equal to $\lambda_{k,k-1} = k\lambda_{10}$, because the service in state k fulfills k channels.

The probabilities $p_0, p_1, p_2, \ldots, p_{k-1}, p_k$ of the states 0, 1, 2,…$k-1$, k are related through the system of Kolmogorov equations for stationary regime of QS (Appendix B). In state k there is not any critical size where loading of the bone leads to the bone fracture. Therefore, the probability p_k of the state k is the probability of the safe loading of the bone denoted by P_S. The solution of Kolmogorov equations (Appendix B) obtains the

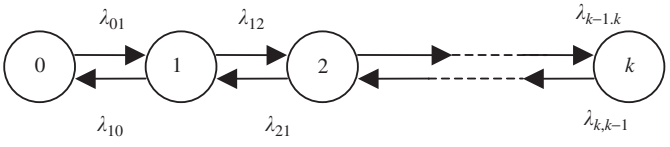

Fig. 4. The graph of the possible states of the queueing system modeling bone loading.

evaluation of probability

$$P_S = \frac{1}{1 + \frac{k!\sigma_{eq}^3}{(k-1)![\sigma_{eq}]^3} + \frac{k!}{(k-2)!}\frac{\sigma_{eq}^6}{[\sigma_{eq}]^6} + \cdots + k!\frac{\sigma_{eq}^{3k}}{[\sigma_{eq}]^{3k}}}. \quad (15)$$

3. Results

According to the calculations of the statically admissible stresses (Appendix D), in two critical sites of bone around a pore where maximum tensile stresses σ_1^+ act, the equivalent stresses are equal to

$$\sigma_{eq} \approx \sigma_1^+ = 3q\frac{1+\chi}{(1-\chi)^2} + q_F\frac{1+\chi}{1-\chi}. \quad (16)$$

Here χ is porosity.

The limited equivalent stresses $[\sigma_{eq}]$ in these critical sites according to assumptions which were considered in part (iii). Evaluation of the tensile stresses in the porous bone region are equal to

$$[\sigma_{eq}] \approx \left[\frac{E_{eff}\sigma_{b1}^3 h_1}{(1+\nu)(\rho_1 - 0.5h_1)}\right]^{0.25}. \quad (17)$$

The probability of safe loading of the bone P_S is defined by the expression (15) after accepting a number of channels $k = 2$ because there are two critical sites in bone. Accordingly

$$P_S = \frac{1}{1 + 2\sigma_{eq}^3/[\sigma_{eq}]^3 + 2\sigma_{eq}^6/[\sigma_{eq}]^6}. \quad (18)$$

Figs. 5 and 6 depicts the results of calculations of possibility of safe loading of femoral neck in areas of porosity. The values used in this analysis are given in Table 1. The values for q_F, α, E_{eff0}, σ_{b10}, ν, were taken as the averaged data from articles by Cowin (1999), Currey (2004) and Zysset (2003). The constants c_1, c_2, c_3 were taken to be equal to average assessments from part 'ii. The effect of porosity'. Values ρ_{10}, h_1 were adapted from data in articles published by Kabel et al. (1999), Zioupos and Currey (1998) and Draper and Goodship (2003).

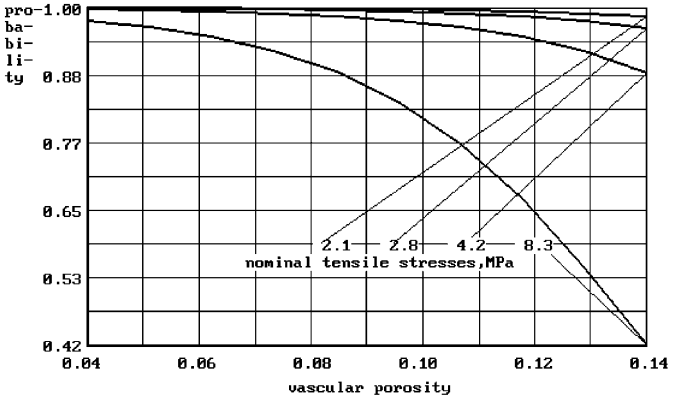

Fig. 5. Predicted probability of safe loading of the femoral neck plotted against the vascular porosity.

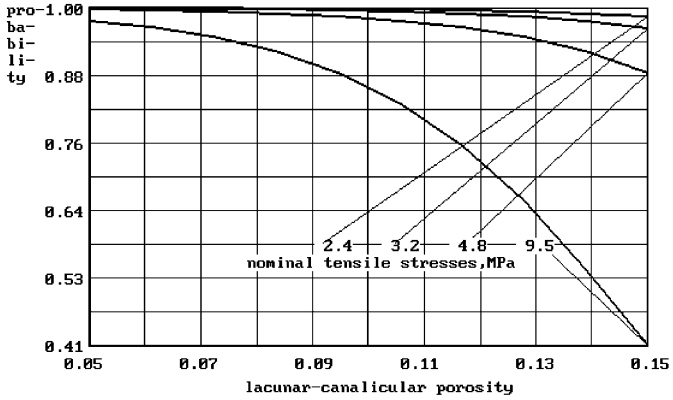

Fig. 6. Predicted probability of safe loading of the femoral neck plotted against the lacunar–canalicular porosity.

According to the calculations; while the nominal tensile stresses acting in bone are below (4.2−4.8) MPa, the probability of safe bone loading is about 0.98 for porosity 0.10 and about 0.9−0.89 for porosity 0.15. The nominal tensile stresses (8.3−9.5) MPa may be considered as critical ones because they lead to sharp drop of probabilities of safe bone loading: to 0.85−0.8 if the porosity is 0.10 and to 0.41−0.4 if the porosity is 0.15. Calculations show existence of the relative safe level of bone loading (if the nominal tensile stresses do not exceed (2.8−3.2) MPa despite the significant bone porosity).

4. Discussion

The goal of the present article was to contribute to the understanding of the occurrence of fractures in the femoral neck. To achieve this goal the following issues were addressed:

(I) criterion for bone fracture taking into consideration the complex state of stress–strains in the porosity zones of the bone was formulated;
(II) tensile stresses around pores in the stretched zone of the bone were evaluated;
(III) the influence of random events on the critical regimes of loading of bone was modeled.

According to the proposed energetic criterion of bone fracture, the fracture occurs when the works done by the tensile stress on the equivalent plastic strains reach the levels of the ultimate work. These levels may be defined from standard mechanical tests for specimens cut out off the critical sites of the bone in the critical directions. The evaluation of the ultimate work from data of bending tests was considered.

By using the momentary effective Young's modulus, the criterion of the bone fracture was extended to the medium described by the equations representing elastic–linear viscous–plastic material. The application of this medium was used for the assessments of the tensile stresses near the

Table 1
Data used for calculations of safe loading of the femoral neck q_F is the pressure of the bone fluid; α is the bone porosity; E_{eff0} is the initial value of the effective Young's modulus; σ_{b10} is ultimate tensile strength of bending specimens in directions of acting the maximum tensile stresses, v is Poison ratio; c_1, c_2, c_3 are constants in expressions (7)–(10), ρ_{10} is initial radius of curvature of the outer surface of bent specimen; h_1 is the height of this specimen

Porosity	q_F (Pa)	α	E_{eff0} (GPa)	σ_{b10} (MPa)	v	c_1	c_2	c_3	ρ_{10} (m)	h_1 (m)
Vascular	0	0.04	15.8	83	0.3	10	10	10	0.2	0.005
Lacunar–canalicular	0.1	0.05	17.5	95	0.3	10	10	10	0.2	0.005

pores while accounting for pore sizes, distribution of the pores and the pressure of the bone liquid.

The influence of the random events on the bone fracture was modeled by QS with refusals. The zones of bones which are critical to possible fractures were simulated by the channels for service of the requirements. The intensities of the fluxes of the random events transfer QS from one possible state to another state are assumed to be inversely proportional to the current equivalent stresses and to the ultimate equivalent stresses. Application of this model obtains the estimations of the probability of safe loading of bone in the stretched regions of the bone porosity. These estimations take into account the levels of the specific tensile loading and the reduction of Young's modulus and ultimate tensile stresses with the increase of the bone porosity.

The introduced fracture criterion explains the following well-known facts. The large strains in sites of bone porosity do not lead to the fracture if the strains are in the compressed zone. The tensile stresses in sites of the bone porosity do not lead to the fracture if the corresponding strains are small. The fractures are always observed in zones of the bone porosity if both tensile stresses and strains are large. In the sites of bone porosity which undergo the extension along two or three mutually perpendicular axes, the fractures are observed for smaller strains than for the sites undergoing uniaxial extension.

Compared to existing methods of prediction of bone fracture, the present method provides better agreement with the observed mechanical behavior of porous regions of bones.

The results obtained provide an explanation of the large variation in probability of hip fracture between the different geographical regions, groups of population, incidents, which have discovered in studies (Kanis et al., 2002; Kanis, 2002a, b). Indeed, the critical correlation between the nominal tensile stresses in bone and its strength depends on many factors: age, gender, weight, race, anthropometrics, physical activity, nourishment, and environment. An established pattern of decrease of the probabilities of safe loading of the femoral neck with increase of bone porosity (Figs. 5 and 6) corresponds to exponential increase in hip fracture probability, as described in studies by Kanis (2002a, b), with increasing of age of men and women (and corresponding decreasing of bone mineral density). The proposed evaluations of the probability of safe bone loading facilitates improved assessments of a dangerous level of osteoporosis considered in review of Kanis (2002b), because they are based on the physical model of failure.

5. Conclusions

Methodology for predicting a probability of safe loading of the femoral neck (without failure) has been demonstrated. This paper focused on modeling of the critical regions of bones by many-channels open QSs with refusals by employing energetic criterion of the bone raptures and the analysis of the stress–strain state around pores in stretched zones of the bone. The limitations of the proposed analysis are in the simplicity of fracture criterion, analysis of stress–strain state of bone, stochastic model of fracture. Further studies are underway to eliminate these limitations.

Appendix A

We suppose that bone material obeys the following relationship for homogeneous, isotropic, elastic–viscous–plastic material (Timoshenko and Goodier, 1970; Kachanov, 1971),

$$\frac{E}{1+v}(\varepsilon_x-\varepsilon/3)+2\left(\mu+\frac{\sigma_{eq}}{3\dot{\varepsilon}_{eq}}\right)(\dot{\varepsilon}_x-\dot{\varepsilon}/3)=\sigma_x-\sigma,$$

$$\vdots \qquad (A.1)$$

$$G\gamma_{zx}+\left(\mu+\frac{\sigma_{eq}}{3\dot{\varepsilon}_{eq}}\right)\dot{\gamma}_{zx}=\tau_{zx}, \qquad (A.2)$$

where E is an arithmetic mean of values of Young's modules in directions of the orthotropic; v is an arithmetic median of values of Poisson's ratios in these directions; $G=E/2(1+v)$; σ_x, …, τ_{zx}, are the normal and shear stresses; $\varepsilon_x,\ldots,\gamma_{zx}$ are the small linear and shear strains; $\dot{\varepsilon}_x,\ldots,\dot{\gamma}_{zx}$ are the linear and shear stain rates; σ_{eq}, ε_{eq}, $\dot{\varepsilon}_{eq}$ are the equivalent stress, the equivalent strain and the equivalent strain rate, respectively; μ is an arithmetic median of values of a dynamic coefficient of a viscosity in directions of orthotropic

$$\varepsilon=\varepsilon_x+\varepsilon_y+\varepsilon_z,$$
$$\sigma=(\sigma_x+\sigma_y+\sigma_z)/3,$$
$$\dot{\varepsilon}=\dot{\varepsilon}_x+\dot{\varepsilon}_y+\dot{\varepsilon}_z.$$

During the loading of the bones in time t it may be accepted that

$$\dot{\varepsilon}_x = \varepsilon_x/t, \quad \dot{\gamma}_{zx} = \gamma_{zx}/t, \quad \dot{\varepsilon} = 0. \tag{A.3}$$

Use the momentary effective Young's module E_{eff} and shear module G_{eff}, defined by the following expressions:

$$E_{\text{eff}} = \frac{2(1+\nu)\sigma_{\text{eq}}}{3\varepsilon_{\text{eq}}}\left[1 + \left(3\mu\frac{\varepsilon_{\text{eq}}}{\sigma_{\text{eq}}} + \frac{\varepsilon_{\text{eq}}}{\dot{\varepsilon}_{\text{eq}}}\right)\Big/ t\right], \tag{A.4}$$

$$G_{\text{eff}} = \frac{E_{\text{eff}}}{2(1+\nu)}. \tag{A.5}$$

Then the correlations between the stresses and the strains in the porosity regions of the bone are similar to the correlations for the elastic material, so that in any short time the bone material can be considered quasi-elastic:

$$\varepsilon_x - \varepsilon/3 = \frac{1+\nu}{E_{\text{eff}}}(\sigma_x - \sigma),$$

$$\vdots \tag{A.6}$$

$$\gamma_{zx} = \frac{1}{G_{\text{eff}}}\tau_{zx}. \tag{A.7}$$

It was assumed that in each loading of the elementary volume of the bone, the plastic strains appear and the equivalent plastic strain e_{eq} is equal to

$$e_{\text{eq}} = \varepsilon_{\text{eq}} p_{\text{pl}}. \tag{A.8}$$

Here ε_{eq} is the equivalent elastic strain in the elementary volume; p_{pl} is the probability of the plastic deformations. According to Hook's law the value ε_{eq} is equal to

$$\varepsilon_{\text{eq}} = \frac{2(1+\nu)\sigma_{\text{eq}}}{3E_{\text{eff}}}. \tag{A.9}$$

Assume

$$p_{\text{pl}} = 0.5W_{\text{e}}/W_{\text{ef}} \approx 0.5\sigma_{\text{eq}}^2/\sigma_{\text{Y}}^2. \tag{A.10}$$

Here W_{e} is the median specific work of the elastic shape deformation of the elementary volume; W_{ef} is the end value of W_{e} when the median value of the effective yield tensile strength σ_{Y} approaches the equivalent stress σ_{eq}. Then the following results are obtained:

$$e_{\text{eq}} = \frac{(1+\nu)\sigma_{\text{eq}}^3}{3E_{\text{eff}}\sigma_{\text{Y}}^2},$$
$$\mathrm{d}e_{\text{eq}} = \frac{(1+\nu)\sigma_{\text{eq}}^2}{E_{\text{eff}}\sigma_{\text{Y}}^2}\mathrm{d}\sigma_{\text{eq}}. \tag{A.11}$$

Substitute into the equalities (2) in the main text above the value $\mathrm{d}e_{\text{eq}}$ from (A.11) and the terms:

$$\beta_1 = \sigma_1^+/\sigma_{\text{eq}}, \quad \beta_2 = \sigma_2^+/\sigma_{\text{eq}},$$
$$\beta_3 = \sigma_3^+/\sigma_{\text{eq}}. \tag{A.12}$$

Then these equalities obtain the assessments of works: W_1, W_2, W_3;

$$W_1 = \frac{(1+\nu)\beta_1\sigma_{\text{eq}}^4}{4E_{\text{eff}}\sigma_{\text{Y}}^2}, \quad W_2 = \frac{(1+\nu)\beta_2\sigma_{\text{eq}}^4}{4E_{\text{eff}}\sigma_{\text{Y}}^2},$$
$$W_3 = \frac{(1+\nu)\beta_3\sigma_{\text{eq}}^4}{4E_{\text{eff}}\sigma_{\text{Y}}^2}. \tag{A.13}$$

Appendix B

The QSs accepted for simulation of loading of the femoral neck are the models of systems for a service of requirements if the requirements arrive in random intervals of time and time intervals for a service are too random (Saaty, 1961; Gross and Harris, 1985). The QSs are dynamic systems. They may be at least in two possible states: state of waiting of requirements and state of their service. The streams of random events transit QS from one possible state in another state. That part of QS, where the requirements are served, is called a channel for service (or server). If the interval of time between two requirements arriving in QS for service is less than the interval of time for their service, QS is busy for service. If the requirement arriving in the busy QS may not remain in the system, such system is a system with refusals. If the requirement arriving in the busy QS may remain in system before its service begins, such QS is the system with queue.

Intensity of fluxes of random events that transit QS from one state into another state is equal to the mean of events in the unit interval of time. Streams of random events are called the simplest fluxes if they are stationary, ordinary and memory-less. The stream is stationary if its intensity does not depend on time. The stream is ordinary if in same time only one event may be occurring. The stream is memory-less if from any time of observation its behavior does not depend on its behavior before. Such stream is called Markovian stream. In the simplest fluxes of random events the distribution function of random events is exponential distribution function

$$F = 1 - \exp(-\lambda t). \tag{B.1}$$

Here t is time, λ is the intensity of process. In exponential distribution, the mean value is equal to the standard deviation.

Let k be the total number of the possibility states of QS, p_i and p_j are probabilities of the states i and j, λ_{ij} is the intensity of the flux of random events that transfers QS from the state i into the state j, λ_{ij} is the intensity of the flux of random events that transits QS from the state j into the state i. Functioning of QS is described by the system of Chapman–Kolmogorov equations, supplied by the normalization condition

$$\frac{\mathrm{d}p_i}{\mathrm{d}t} = \sum_{\substack{j=1 \\ j\neq i}}^{k} p_j\lambda_{ji} - p_i\sum_{\substack{j=1 \\ i\neq i}}^{k}\lambda_{ij},$$
$$i = \overline{1,k}, \quad \sum_{i=1}^{k} p_i = 1. \tag{B.2}$$

The amount of the differential equations is equal to the amount of states of QS. In the right-hand part of each differential equation amount of terms is equal to the amount of states connected with the considered state plus one. The amount of the positive terms is equal to the amount of the states of QS that may be transited in the considered state. Amount of the negative terms is equal to the states QS in which the considered state may be transited.

Let the QS with the graph of the possible states in Fig. 4 works in stationary regime. Then the probabilities p_0, p_1, $p_2,\ldots, p_{k-1}, p_k$ of the states 0, 1, 2,…, $k-1$, k are connected by following equations:

$$\begin{aligned} &-p_0\lambda_{01} + p_1\lambda_{10} = 0,\\ &p_0\lambda_{01} - p_1(\lambda_{10}+\lambda_{12}) + p_2\lambda_{21} = 0,\\ &\quad\vdots\\ &p_{k-1}\lambda_{k-1.1} - p_k\lambda_{k.k-1} = 0, \end{aligned} \tag{B.3}$$

$$p_0 + p_1 + \cdots + p_k = 1. \tag{B.4}$$

The solution of Eqs. (B.3) and (B.4) yields

$$\begin{aligned} &p_0 = \frac{1}{1+\frac{\lambda_{01}}{\lambda_{10}}+\frac{\lambda_{01}\lambda_{12}}{\lambda_{10}\lambda_{21}}+\cdots+\frac{\lambda_{01}\lambda_{12}\cdots\lambda_{k-1.k}}{\lambda_{10}\lambda_{21}\cdots\lambda_{k.k-1}}},\\ &p_1 = p_0\frac{\lambda_{01}}{\lambda_{10}},\\ &\quad\vdots\\ &p_k = p_0\frac{\lambda_{01}\lambda_{12}\cdots\lambda_{k-1.k}}{\lambda_{10}\lambda_{21}\cdots\lambda_{k.k-1}}. \end{aligned} \tag{B.5}$$

Use the substitutions from section 'Methods', division (iv). The probability of safe loading of the femoral neck:

$$\begin{aligned} &\lambda_{01} = \lambda_{12} = \cdots = \lambda_{k-1.k}, \quad \lambda_{21} = 2\lambda_{10},\\ &\lambda_{32} = 3\lambda_{10}\ldots\lambda_{k.k-1} = k\lambda_{10}. \end{aligned} \tag{B.5′}$$

Then the probability of the state k is equal to

$$p_k = \frac{1}{1+\frac{k!}{(k-1)!}\frac{\lambda_{10}}{\lambda_{01}}+\frac{k!}{(k-2)!}\left(\frac{\lambda_{10}}{\lambda_{01}}\right)^2+\cdots+k!\left(\frac{\lambda_{10}}{\lambda_{01}}\right)^k}. \tag{B.6}$$

Appendix C

Assume that the bent specimens have a square cross-section and the plane of the bending is parallel to the direction 1 where the maximum tensile stresses σ_1^+ act. Then the limited equivalent plastic strain $[e_{eq}]_1$ and stresses σ_1^+ may be evaluated by the equalities:

$$[e_{eq}]_1 = h_1/(2\rho_1 - h_1), \quad \sigma_1^+ = \sigma_{eq}. \tag{C.1}$$

Here h_1 is the initial height of the specimen; ρ_1 is the radius of the curvature of the outer surface of the specimen in the moment of onset of the rapture. The tensile stresses in two perpendicular directions σ_2^+ and σ_3^+ in the bent specimens may be assumed to be negligible. One can assume that in such a specimen, the connections between e_{eq} and σ_{eq} are described by the equality:

$$\sigma_{eq} = \sigma_{b1}e_{eq1}/[e_{eq}]_1. \tag{C.2}$$

Then

$$\begin{aligned} [W]_1 &= \int_0^{[e_{eq}]_1}\sigma_1^+\,de_{eq} = \int_0^{[e_{eq}]_1}\sigma_{eq}de_{eq1}\\ &= \sigma_{b1}\frac{h_1}{4(\rho_1 - 0.5h_1)}. \end{aligned} \tag{C.3}$$

Similarly

$$\begin{aligned} &[W]_2 \approx \frac{\sigma_{b2}h_2}{4(\rho_2 - 0.5h_2)} \text{ and}\\ &[W]_3 \approx \frac{\sigma_{b3}h_3}{4(\rho_3 - 0.5h_3)}. \end{aligned} \tag{C.4}$$

Appendix D

The assumed distributions of the stresses in the bone porosity zone is described below. In region 1, in the system of the cylindrical coordinates r, ϑ, z with the origin in the center of the circle circumscribing the pore, the following stresses are acting:

$$\begin{aligned} &\sigma_r = \sigma_\vartheta = -q_F,\\ &\sigma_z = \tau_{r\theta} = \tau_{\vartheta z} = \tau_{rz} = 0. \end{aligned} \tag{D.1}$$

Here σ_r is the radial stress, σ_ϑ is the circumferential stress, σ_z is the axial stress; $\tau_{r\vartheta}, \tau_{rz}, \tau_{z\theta}$ are the corresponding shear stresses; ϑ is the angle depicted in Figs. 2 and 3. In region 3 of the x, y, z space, with the axis x directed along the direction of action of the nominal tensile stresses q, the following stresses are acting:

$$\sigma_x = q, \quad \sigma_y = \sigma_z = \tau_{xy} = \tau_{yz} = \tau_{zx} = 0. \tag{D.2}$$

The expressions (D.1) and (D.2) satisfy the static boundary condition of the linear tension of the stripe-shape region away from the pore and of the uniform pressure on the inner surface of the pore. These stresses satisfy the differential equations of equilibrium without accounting for the inertial forces.

$$\frac{\partial\sigma_r}{\partial r} + \frac{\sigma_r - \sigma_\vartheta}{r} + \frac{\partial\tau_{r\vartheta}}{r\partial\vartheta} = 0, \tag{D.3}$$

$$\frac{\partial\sigma_\vartheta}{r\partial\vartheta} + \frac{\partial\tau_{r\vartheta}}{\partial r} + \frac{2\tau_{r\vartheta}}{r} = 0. \tag{D.4}$$

The expressions (D.1) and (D.4) lead to following conditions of the statically admission of the stress discontinuity on the borders $r = a$ and $r = R$ between region 2 and regions 1 and 3:

$$r = a, \quad \sigma_r = -q_F, \quad \tau_{r\vartheta} = 0, \tag{D.5}$$

$$r = R, \quad \sigma_r = 0.5q(1+\cos 2\vartheta), \quad \tau_{r\vartheta} = -0.5q\sin 2\vartheta. \tag{D.6}$$

In order to find the stress distribution in region 2 the solution of the elastic equilibrium of the stretched stripe

with a hole was used (Timoshenko and Goodier, 1970):

$$\sigma_r = \frac{1}{r}\frac{\partial \Phi}{\partial r} + \frac{1}{r^2}\frac{\partial^2 \Phi}{\partial \vartheta^2}, \quad \sigma_\vartheta = \frac{\partial^2 \Phi}{\partial r^2}, \tag{D.7}$$

$$\tau_{r\vartheta} = \frac{1}{r^2}\frac{\partial \Phi}{\partial \vartheta} - \frac{1}{r}\frac{\partial^2 \Phi}{\partial r \partial \vartheta}, \tag{D.8}$$

where

$$\Phi = \left(Ar^2 + Br^4 + \frac{C}{r^2} + D\right)\cos 2\vartheta + E\ln r + Kr^2. \tag{D.9}$$

Here the values A, B, C, D, E, K are the arbitrary constants. The expressions (D.7) and (D.8) satisfy the differential equations of the equilibrium and the conditions of the compatibility of the strains.

In order to simplify the solution the constants E, K were obtain from the parts of the conditions (D.5) and (D.6)

$$\begin{aligned} &\text{at } r = a, \quad \sigma_r = -q_F, \\ &\text{at } r = R, \quad \sigma_r = 0.5q. \end{aligned} \tag{D.10}$$

Then the distribution of the stresses is described by the equalities

$$\sigma_r = -\left(2A + \frac{6C}{r^4} + \frac{4D}{r^2}\right)\cos 2\vartheta + 0.5q\frac{1 - a^2/r^2}{1 - a^2/R^2} - q_F\frac{R^2/r^2 - 1}{R^2/a^2 - 1}, \tag{D.11}$$

$$\sigma_\vartheta = \left(2A + 12Br^2 + \frac{6C}{r^4}\right)\cos 2\vartheta + 0.5q\frac{1 + a^2/r^2}{1 - a^2/R^2} + q_F\frac{R^2/r^2 + 1}{R^2/a^2 - 1}, \tag{D.12}$$

$$\tau_{r\vartheta} = \left(2A + 6Br^2 - \frac{6C}{r^4} - 2\frac{D}{r^2}\right)\sin 2\vartheta, \tag{D.13}$$

$$\sigma_z = \tau_{rz} = \tau_{z\vartheta} = 0. \tag{D.14}$$

Using the conditions (D.5) and (D.6) we obtain four linear equations for the definition constants A, B, C, D.

The maximum tensile stresses σ_1^+ are the circumferential stresses σ_ϑ in the elementary volumes at the upper and low points of the diameter of the circumscribed circle, where $r = a$; $\vartheta = \pm\pi/2$. Here

$$\sigma_\vartheta = \sigma_1^+ = 3q\frac{1 + a^2/R^2}{(1 - a^2/R^2)^2} + q_F\frac{1 + a^2/R^2}{1 - a^2/R^2}. \tag{D.15}$$

In these elementary volumes other tensile stresses are negligible and the equivalent stress is approximately equal to

$$\sigma_{eq} \approx \sigma_\vartheta = \sigma_1^+. \tag{D.16}$$

Assuming the ratio $\chi = (a/R)^2$ is an evaluation of the bone porosity, we obtain the influence of bone porosity on the level of the equivalent stresses according to (D.15).

Appendix E

Consider the correspondence between our fracture criterions (1) described in the main text, to published data of mechanical tests in tension, torsion and bending, for metals, alloys, polymers. The tested material is assumed to be homogenous, isotropic, and subjected to work hardening. The work hardening of material is described by the equality:

$$\sigma_Y = Be_{eq}^n \dot{e}_{eq}^m, \tag{E.1}$$

where B, n and m are constants of the tested material in a given temperature and velocity conditions of the tests; e_{eq} and $\dot{e}_{eq}$ are the current equivalent plastic strain and equivalent strain rate, respectively. Assume in the equality (E.1) that $\dot{e}_{eq} \approx e_{eq}/t$, where t is time from beginning of deformation.

In tension tests of cylindrical specimens, the highest tensile stresses acting in the smallest cross-section of a specimen and denoted by σ_1^+ are equal to the yield stress σ_Y, the tensile stresses in other mutually perpendicular directions are negligible ($\sigma_2^+ = \sigma_3^+ = 0$); the equivalent strain is equal to $e_{eq} = \ln(A_0/A)$, where A_0 is an initial area of cross-section of a specimen, and A is a current area of the smallest cross-section of an extending specimen. In torsion tests of cylindrical specimens the highest tensile stresses are: $\sigma_1^+ = \sigma_Y/\sqrt{3}$, the tensile stresses in other mutually perpendicular directions are negligible: $\sigma_2^+ = \sigma_3^+ = 0$.

In bending tests of wide sheet specimens the highest tensile stresses σ_1^+ acting in longitudinal direction are $\sigma_1^+ = 2\sigma_Y/\sqrt{3}$; the tensile stresses acting in transverse direction are equal to $\sigma_2^+ = \sigma_Y/\sqrt{3}$; the tensile stresses acting in direction of the normal to a specimen surface are zero. The ultimate works done of tensile stresses are equal, according to the equality (E.1) and the expressions (2) in the main text

$$[W] = \begin{cases} \int_0^{e_E^*} \sigma_1^+ \, de_{eq} = \int_0^{e_E^*} \sigma_Y \, de_{eq} = \frac{B}{(1+n+m)t^m}\left(e_E^*\right)^{n+m+1} & \text{in tension tests,} \\ \int_0^{e_T^*} \sigma_1^* \, de_{eq} = \frac{1}{\sqrt{3}}\int_0^{e_T^*} \sigma_Y \, de_{eq} = \frac{B}{(1+n+m)\sqrt{3}t^m}\left(e_T^*\right)^{n+m+1} & \text{in torsion tests,} \\ \int_0^{e_B^*} (\sigma_1^+ + \sigma_2^*) de_{eq} = \sqrt{3}\int_0^{e_B^*} \sigma_Y \, de_{eq} = \frac{\sqrt{3}B}{(1+n+m)t^m}\left(e_B^*\right)^{n+m+1} & \text{in bending tests.} \end{cases} \tag{E.2}$$

Here e_E^*, e_T^*, e_B^* are the limited equivalent strains in tension tests, torsion tests and bending tests, respectively. These strains are equal to:

$$e_E^* = \ln\frac{1}{1-\psi}, \quad e_E^* = \tan\varphi,$$
$$e_B^* = h_1/(2\rho_1 - h_1), \tag{E.3}$$

where ψ is the relative reduction of a cross-section of a specimen; φ is the limited angle of twirled specimen; h_1 is the initial height of the bending specimen; ρ_1 is the radius of the curvature of the outer surface of the bending specimen in the onset of the rapture.

Assume the absolute temperature of deformed specimens less than $0.4T_m$, where T_m is the absolute temperature of melting, and $m = 0$. According to the accepted fracture criterion (1) of constancy of the limited work done by tensile stresses, the limited strains in tension tests, torsion tests and bending tests are related as follows:

$$e_T^*/e_E^* = (\sqrt{3})^{1/(1+n)},$$
$$e_B^*/e_E^* = (1/\sqrt{3})^{1/(1+n)}. \tag{E.4}$$

For a common range of constant n: $n = 0 - 0.35$ the relations e_T^*/e_E^* and e_B^*/e_E^* are

$$e_T^*/e_E^* = 1.5 - 1.73,$$
$$e_B^*/e_E^* = 0.577 - 0.66. \tag{E.5}$$

These assessments correspond to published data of mechanical tests for the most of known metals, alloys and polymers (Gere and Timoshenko, 2000; Kannine et al., 1969; Kausch et al., 1973) if plastic deformation of specimens does not lead to a phase transformations in the structure of the specimens.

References

Bagge, M., 2000. A model of bone adaptation as an optimization process. Journal of Biomechanics 33, 1349–1357.

Brazier, J.E., Green, C., Kanis, J.A., 2002. A systematic review of health state utility values for osteoporosis-related conditions. Osteoporosis International 13, 768–776.

Cowin, S.C., 1999. Bone poroelasticity. Journal of Biomechanics 32, 217–238.

Crabtree, N.J., Kroger, H., Martin, A., Pols, H.A.P., Lorenc, R., Nijs, J., Stepan, J.J., Falch, J.A., Miazgowski, T., Grazio, S., Raptou, P., Adams, J., Collings, A., Khaw, K.-T., Rushton, N., Lunt, M., Dixon, A.K., Reeve, J., 2002. Improving risk assessment: hip geometry, bone mineral distribution and bone strength in hip fracture cases and controls. The EPOS study. Osteoporosis International 13, 48–54.

Cummings, S.R., Black, D.M., Nevitt, M.C., Browner, W., Cauley, J., Ensrud, K., Genant, H.K., Palermo, L., Scott, J., Vogt, T.M., 1993. Bone density at various sites for prediction of hip fractures. Lancet 341, 72–75.

Currey, J.D., 2004. Tensile yield in compact bone is determined by strain, post-yield behaviour by mineral content. Journal of Biomechanics 37, 549–556.

Dargent-Molina, P., Favier, F., Grandjean, H., Baudoin, C., Schott, A.M., Hausherr, E., Meunier, P.J., Breart, G., 1996. Fall related factors and risk of hip fracture: the EPIDOS prospective. Lancet 348, 145–149.

Dong, X.N., Guo, X.E., 2004. The dependence of transversely isotropic elasticity of human femoral cortical bone on porosity. Journal of Biomechanics 37, 1281–1287.

Draper, E.R.C., Goodship, A.E., 2003. A novel technique for four-point bending of small bone samples with semi-automatic analysis. Journal of Biomechanics 36, 1497–1502.

Duboeuf, F., Hans, D., Schott, A.M., Kotzki, P.O., Favier, F., Marcelli, C., Meunier, P.J., Delmas, P.D., 1997. Different morphometric and densitometric parameters predict cervical and trochanteric hip fracture: the EPIDOS study. Journal of Bone and Mineral Research 12 (11), 1895–1902.

Ganguly, P., Moore, T.L.A., Gibson, L.J., 2004. A phenomenological model for predicting fatigue life in bovine trabecular bone. Transactions of the ASME—Journal of Biomechanical Engineering 126, 330–339.

Gere, J.M., Timoshenko, S.P., 2000. Mechanics of Materials, fifth ed. Chapman & Hall, London, 808pp.

Gross, D., Harris, C.M., 1985. Fundamentals of Queueing Theory, second ed. Wiley, New York.

Haddock, S.M., Yeh, O.C., Mummaneni, P.V., Rosenberg, W.S., Keaveny, T.M., 2004. Similarity in the fatigue behavior of trabecular bone across site and species. Journal of Biomechanics 37, 181–187.

Homminga, J., Mccreadie, B.R., Weinans, H., Huiskes, R., 2003. The dependence of the elastic properties of osteoporotic cancellous bone on volume fraction and fabric. Journal of Biomechanics 36, 1461–1467.

Kabel, J., van Rietbergen, B., Odgaard, A., Huiskes, R., 1999. Constitutive relationships of fabric, density, and elastic properties in cancellous bone architecture. Bone 25 (4), 481–486.

Kachanov, L.M., 1971. Foundations of the Theory of Plasticity. Noth-Holland, Amsterdam.

Kanis, J.A., 2002a. Diagnosis of osteoporosis and assessment of fracture risk. Lancet 359, 1929–1936.

Kanis, J.A., 2002b. Assessing the risk of vertebral osteoporosis, Review article. Singapore Medical Journal 43 (2), 100–105.

Kanis, J.A., Johnell, O., De Laet, C., Jonsson, B., Oden, A., Ogelsby, A.K., 2002. International variations in hip fracture probabilities: implications for risk assessment. Journal of Bone and Mineral Research 17 (7), 1237–1246.

Kannine, M.F., Adler, W.F., Rosenfeld, A.R., Jaffee, R.J. (Eds.), 1969. Inelastic Behavior of Solids. McGraw-Hill, New York, p. 641.

Kartoge, S., Dalzell, N., Loveridge, N., Beck, T.J., Khaw, K.-T., Reeve, J., 2003. Effects of gender, anthropometric variables, and aging on the evolution of hip strength in men and women aged over 65. Bone 32, 561–570.

Kausch, H.H., Hassell, J.A., Jaffee, R.J. (Eds.), 1973. Deformation and Fracture of High Polymers. Plenum, New York.

Keyak, J.H., Rossi, S.A., 2000. Prediction of femoral fracture load using finite element models: an examination of stress- and strain-based failure theories. Journal of Biomechanics 33, 209–214.

Malik, C.L., Stover, S.M., Martin, R.B., Gibeling, J.C., 2003. Equine cortical exhibits rising R-curve fracture mechanics. Journal of Biomechanics 36, 191–198.

Mayhew, P.M., Thomas, C.D., Clement, J.G., Loveridge, N., Beck, T.J., Bonfield, W., Burgoyne, C.J., Reeve, J., 2005. Relation between age, femoral neck cortical stability, and hip fracture risk. Lancet 366, 129–135.

Morgan, E.F., Bayraktar, H.H., Keaveny, T.M., 2003. Trabecular bone modulus-density relationships depend on anatomic site. Journal of Biomechanics 36, 897–904.

Nalla, R.K., Stolken, J.S., Kinney, J.H., Ritchie, R.O., 2005. Fracture in human cortical bone: local fracture criteria and toughening mechanisms. Journal of Biomechanics 38, 1517–1525.

Norman, T.L., Vashishth, D., Burr, D.B., 1995. Fracture toughness of human bone under tension. Journal of Biomechanics 28, 309–320.

Ota, T., Yamamoto, I., Morita, R., 1999. Fracture simulation of the femoral bone using the finite-element method: how a fracture initiates and proceeds. Journal of Bone and Mineral Metabolism 17, 108–112.

Pietruszczak, S., Inglis, D., Pande, G.N., 1999. A fabric-dependent fracture criterion for bone. Journal of Biomechanics 32, 1071–1079.

Rajapakse, C.S., Thomsen, J.S., Ortiz, J.S.E., Wimalawansa, S.J., Ebbesen, E.N., Mosekilde, L., Gunaratne, G.H., 2004. An expression relating breaking stress and density of trabecular bone. Journal of Biomechanics 37, 1241–1249.

Saaty, T.L., 1961. Elements of Queueing Theory with Applications. McGraw-Hill, New York.

Smit, T.H., Huyghe, J.M., Cowin, S.C., 2002. Estimation of the poroelastic parameters of cortical bone. Journal of Biomechanics 35, 829–835.

Testi, D., Viceconti, M., Baruffaldi, F., Cappello, A., 1999. Risk of fracture in elderly patients: a new predictive index based on bone mineral density and finite element analysis. Computer Methods and Programs in Biomedicine 60, 23–33.

Testi, D., Viceconti, M., Cappello, A., Gnudi, S., 2002. Prediction of hip fracture can be significantly improved by a single biomedical indicator. Annals of Biomedical Engineering 30, 801–807.

Testi, D., Cappello, A., Sgallari, F., Rumpf, M., Viceconti, M., 2004. A new software for prediction of femoral neck fractures. Computer Methods and Programs in Biomedicine 75, 141–145.

Timoshenko, S.P., Goodier, J.N., 1970. Theory of Elasticity, third ed. McGraw-Hill, New York.

Wirtz, D.C., Pandort, T., Portheine, F., Radermacher, K., Schiffers, N., Prescher, A., Weichert, D., Niethard, F.U., 2003. Concept and development of an orthotropic FE model of the proximal femur. Journal of Biomechanics 36, 289–293.

Yeni, Y.N., Fyhrie, D.P., 2003. A rate-dependent microcrack-bridging model that can explain strain rate depency of cortical bone apparent yield strength. Journal of Biophysics 36, 1343–1353.

Zioupos, P., Currey, J.D., 1998. Changes in the stiffness, strength, and toughness of human cortical bone with age. Bone 22 (1), 57–66.

Zysset, P.K., 2003. A review of morphology-elasticity relationships in human trabecular bone: theories and experiments. Journal of Biomechanics 36, 1469–1485.